Nanoscale Spectroscopic Imaging of Organic Semiconductor Films by Plasmon-Polariton Coupling

D. Zhang,[1,†] U. Heinemeyer,[2] C. Stanciu,[1] M. Sackrow,[1] K. Braun,[1] L. E. Hennemann,[1] X. Wang,[1] R. Scholz,[3] F. Schreiber,[2] and A. J. Meixner[1,*]

[1]*Institute of Physical and Theoretical Chemistry, University of Tübingen, D-72076 Tübingen, Germany*
[2]*Institute of Applied Physics, University of Tübingen, D-72076 Tübingen, Germany*
[3]*Walter Schottky Institute and Physics Department, Technical University of Munich, D-80333 München, Germany*
(Received 27 February 2009; published 3 February 2010)

Tip-enhanced near-field optical images and correlated topographic images of an organic semiconductor film (diindenoperylene, DIP) on Si have been recorded with high optical contrast and high spatial resolution (17 nm) using a parabolic mirror with a high numerical aperture for tip illumination and signal collection. The DIP molecular domain boundaries being one to four molecular layers (1.5–6 nm) high are resolved topographically by a shear-force scanning tip and optically by simultaneously recording the 6×10^5 times enhanced photoluminescence (PL). The excitation is 4×10^4 times enhanced and the intrinsically weak PL-yield of the DIP-film is 15-fold enhanced by the tip. The Raman spectra indicate an upright orientation of the DIP molecules. The enhanced PL contrast results from the local film morphology via stronger coupling between the tip plasmon and the exciton-polariton in the DIP film.

Because of their exciting electronic, optical, and optoelectronic properties, organic semiconductor films are extensively studied for applications in solar cells, organic light emitting diodes, and organic field-effect transistors [1,2]. Diindenoperylene (DIP) is one of the promising organic semiconductor materials. If deposited under suitable conditions on Si oxide or ITO, it forms closed films with high structural order and has a relatively large exciton diffusion length of about 100 nm along the growth direction on ITO [3,4]. The electronic properties of thin films are usually different from the monomer or bulk crystal properties; moreover, they depend strongly on the microscopic film morphology, such as grain boundaries. The need for understanding and exploiting these phenomena led to a large number of investigations in scanning probe microscopy combined with confocal microscopy [5]. However, the quantitative spectroscopic measurement of local optical properties of organic semiconductor surfaces with a resolution matching molecular domains has been plagued by a lack of contrast, sensitivity, or spatial resolution. To address this challenging issue, we have carried out tip-enhanced spectroscopic measurements on a DIP thin film employing our home-built parabolic mirror assisted near-field optical microscope [6].

A sharp laser-illuminated Au tip is used as an optical antenna approaching closely to the sample surface, confining the excitation field to a subdiffraction volume at the tip apex and retrieving emitted or scattered photons to the far field for detection. A sensitive feedback based on tunneling current [7] or mechanical force [8] prevents the tip from crashing into the surface and allows for recording simultaneously the topography and the correlated chemical information via Raman spectroscopy [7]. The topographic

resolution of this technique can reach a few nanometers, whereas the optical resolution is essentially determined by the apex size of the antenna tip [9].

Thirty nm thick DIP films were deposited on Si(100) covered with native oxide [10]. Tip-enhanced spectroscopic measurements are performed by radially illuminating the apex of an electrochemically etched sharp Au tip with $\lambda = 632.8$ nm He-Ne laser light polarized along the tip shaft [Fig. 1(a)]. In contrast to conventional near-field optical microscopes, we used a parabolic mirror for illumination and signal collection [Fig. 1(b)] which are performed from the top of the sample under perfect diffraction and polarization conditions. Hence, no restriction applies with respect to the conductivity or transparency of the sample substrate [11].

In Fig. 2(a), a near-field optical image of the DIP film is shown with the simultaneously recorded topography, revealing the well-known DIP film morphology with stepped
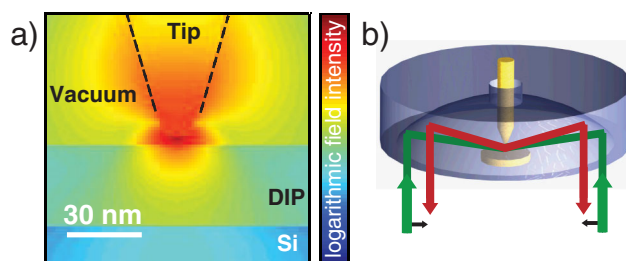

FIG. 1 (color online).   (a) Calculated field intensity distribution when an Au tip is placed 3 nm above a 30 nm DIP film. The intensity is plotted on a logarithmic scale. (b) Illumination (green upright arrows) and optical signal collection (red downward arrows) by the parabolic mirror.

terraces [10]. Most of the domains exhibit step heights of 1.5–1.8 nm, in accordance with upright-oriented DIP molecules defining a lattice constant along the substrate normal of 1.65 nm [see Fig. 2(b)] [10]. Some exceptionally high dots appearing in the topography, such as the one labeled as 1, are probably dust particles from the ambient experimental condition. The near-field optical image shows bright lines, spots, and dark regions appearing at first glance like random features. However, a thorough comparison with the topography reveals that the bright features correlate with most of the DIP domain boundaries, such as the regions labeled as 2, 3, and 4. Moreover, enhanced optical contrast is observed in regions where no molecular step is revealed in the topography, such as region 5. The optical signal from bright regions is about four times higher than that of dark regions and does not depend significantly on the step height. The blue vertical arrows in Fig. 2(b) point out a terrace boundary of one molecular height where a sharp optical signal with a FWHM of ≈17 nm (red horizontal arrows) is resolved, indicating an optical resolution of at least 17 nm.

To investigate the nature of the tip-enhanced spatially resolved optical features, spectroscopic measurements were performed. Figure 3(a) shows the spectrum (II) recorded without a tip. The dominant Raman line at 520 cm^{-1} is the optical phonon of the Si substrate. The broader feature around 960 cm^{-1} arises from the density of states of two phonons in Si [12]. The contribution of the DIP film is barely visible, consisting of a weak PL background with a maximum at 1575 cm^{-1} (1.76 eV). Upon approaching the Au tip close to the DIP film, an intense tip-enhanced signal appears (spectrum III), consisting of a broad PL background and distinct Raman lines. The

Raman lines of the Si substrate lying 30 nm beneath the DIP surface appear weaker due to the strongly reduced field enhancement. The tip-enhanced Raman bands [Fig. 3(a) IV] at 1291, 1401, 1466, and 1615 cm^{-1} correspond to far-field measured and calculated breathing modes of DIP within deviations of a few cm^{-1} [13,14]. Crystalline DIP films exhibit strongly uniaxial anisotropic properties with the largest component of the dielectric tensor along a direction inclined by approx. 17° against the substrate normal [15]. In Raman spectroscopy, the scattering cross sections are proportional to $|\vec{e}_s \cdot \overleftrightarrow{R} \cdot \vec{e}_i|^2$, where $\vec{e}_i$ and $\vec{e}_s$ are the polarization directions of the incident and scattered fields, and $\overleftrightarrow{R}$ is the Raman tensor (see supplementary material [16]). The near-field below the tip apex is oriented along the substrate normal so that it couples efficiently to the largest element of the
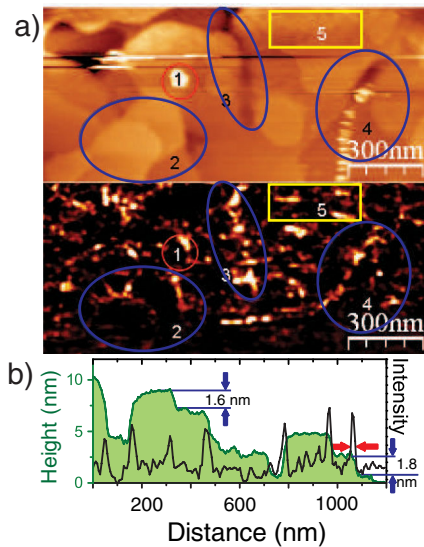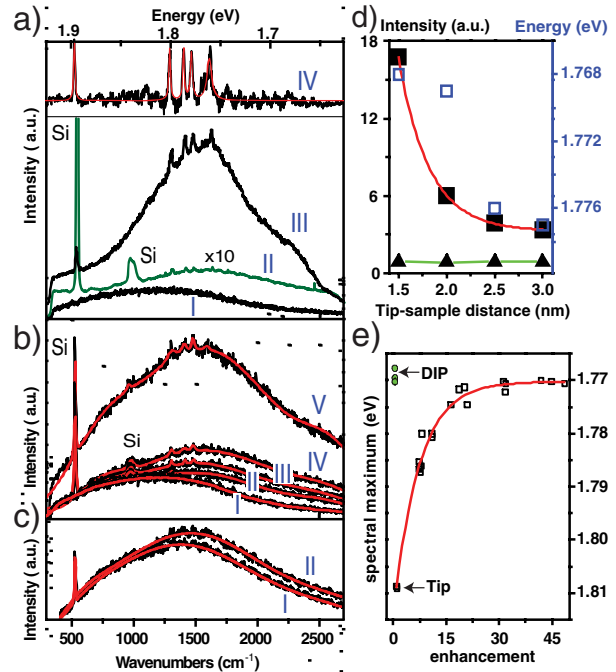
FIG. 3 (color online). (a) Confocal far-field PL-spectrum (I) of a tip alone integrated for 10 s , (II) of DIP film integrated for 900 s, and (III) tip-enhanced spectrum integrated for 10 s at a tip-DIP distance of 3 nm. Excitation power: 170 μW. (IV) Tip-enhanced Raman spectrum obtained from (III) after subtraction of PL-background with fitted spectrum (red curve). (b) Spectra collected at different tip-sample distances. II, 3 nm; III, 2.5 nm; IV, 2 nm; V, 1.5 nm and I: spectrum of tip alone. Integration time: 10 s. (c) PL spectra, (I) from inside a domain and (II) from a domain edge. Tip-sample distance: 3 nm. Excitation power: 170 μW. Acquisition time: 30 s. (d) Intensity of the Si Raman line (triangles), enhancement (closed squares), and energy shift (open squares) of the PL spectra as a function of tip-sample distance. (e) Energetic shift of the spectral maximum as a function of the total signal enhancement for different tips and days (empty squares). For comparison, the spectral maximum from the confocal far-field spectra of DIP are included (green circles).

FIG. 2 (color online). (a) Simultaneously recorded topographic (upper panel) and near-field optical images (lower panel). Scan area: 1.5 × 0.7 μm². Laser power: 170 μW. Tip-sample distance: 3 nm. (b) Line profile through the topographic image with its correlated optical intensity.

Raman tensor corresponding to the long axis of the DIP-molecule. Therefore, the C-C breathing modes are selectively excited giving the Raman patterns observed in the tip-enhanced Raman spectroscopy (TERS) spectrum [17].

In most TERS investigations, the dispersive PL background is of minor interest. However, in our spectra, it dominates the observed intensity so that it is the key to a deeper understanding of the influence of surface morphology on the DIP optical properties. The absorption spectrum excited with a polarization perpendicular to the sample surface shows distinct vibronic lines at 2.25, 2.42, and 2.59 eV [15], giving PL bands at 2.14, 1.96, and 1.77 eV [18]. The two higher lying PL bands cannot be excited by the He-Ne laser. Nevertheless, in the electronic ground state, the first vibronic levels of typical Raman-active breathing modes around 0.17 eV are still thermally occupied with a probability of about 10^{-3}. Starting from these vibronic levels, a further weak resonance is expected around 2.09 eV. The off-resonant excitation with our laser results in the PL band around 1.76 eV shown in Fig. 3(a) (III).

Spectra collected as a function of tip-sample distances in the range from 3 nm to 1.5 nm [see Fig. 3(b)] reveal a steeply increasing PL intensity when approaching the sample to the tip, accompanied by a red shift of the PL maximum, whereas the positions of the DIP Raman lines remain constant. The PL spectrum collected from the Au tip alone is shown in Figs. 3(a) and 3(b) as curve I with a maximum at 1225 cm^{-1} (1.807 eV). It is typical for our Au tips and serves as a reference for estimating the contribution of the tip PL to the distance-dependent spectra II–V in Fig. 3(b). They show clearly different spectral shapes and intensities as compared to the tip spectrum. This indicates that these spectra involve PL contributions from both tip and DIP film. In Fig. 3(e), the maxima of several distance-dependent spectra (different days with different tips) are plotted against the total signal enhancement, revealing an asymptotic approach from the tip PL maximum towards the DIP PL maximum. Therefore, we conclude that the DIP PL dominates the spectra at close tip-sample distances. A careful fitting of the spectra shown in Fig. 3(b) reveals also a slight red shift of the DIP PL from 1.787 to 1.767 eV [blue open squares in Fig. 3(d), see supplementary material [16]]. Recently, Pettinger *et al.* [9] have reported a comparable red shift from 1.882 to 1.826 eV and an intensity increase of the tip-enhanced Raman spectra when reducing the tip-sample distance from 5 to 1 nm towards a layer of guanine/ClO_4^- adsorbed on an Au(111) crystal surface, assigned to a strongly distance-dependent plasmon coupling between Au tip and Au surface interpreted by a free electron gas model [19].

Finite domain time domain simulations of the time-averaged field distribution for our tip-sample configuration [Fig. 1(a)] reveal a high field enhancement in the gap between the Au tip and the DIP film resulting from the efficient coupling of a localized plasmon in the tip apex and a respective polarization in the DIP film just below the gap (see supplementary material [16]). The incident radially polarized light field induces a coherent oscillation of the conduction electrons in the tip along the axis, leading to a local field enhancement in and around the tip apex, in the tip-DIP gap, and in the DIP film underneath. Hence, we have a similar situation as found in the case of an Au tip above an Au(111) crystal where the tip plasmon and the localized surface plasmons are coupled by the gap field [20]. In analogy to the conduction electrons in gold, in the highly ordered DIP film, the π electrons provide the major contribution of the dielectric constant [15,17]. Therefore, in response to the plasmon oscillation in the tip, we have a coherent local oscillation of the π electrons in the film leading to an exciton-polariton strongly coupled to the gap field. Integrating the PL intensities of spectra II and III in Fig. 3(a), one can derive that the PL intensity in the TERS spectrum is about 2600 times stronger. In addition, the intensity enhancement in the gap is restricted to an area of about $A = 227$ nm^2, much smaller than the area of the far-field focus with a diameter of about 260 nm, corresponding to $A = 5.3 \times 10^4$ nm^2. Hence, we find an average enhancement factor in the first molecular layer under the tip of 6×10^5. To explain the origin of such a high PL enhancement, one must compare for the tip-enhanced case and for the confocal case the excitation rate Γ_{exc}, and the balance between the radiative decay rate Γ_r and the nonradiative decay rate Γ_{nr}, since the PL intensity is proportional to $\Gamma_{exc}[1 - \Gamma_{nr}/(\Gamma_r + \Gamma_{nr})]$, the term in brackets being the PL yield. The PL in DIP films results from the radiative decay of Frenkel excitons created locally in the surface layer of the molecular film. An exciton has a transition dipole $\mathbf{D}_{exc} = 8.2$ D [17] oriented along the long axis of the DIP molecules. The excitation rate Γ_{exc} is proportional to $|\mathbf{D}_{exc} \cdot \mathbf{E}_{exc}|^2$ where $\mathbf{E}_{exc}$ is the effective excitation field at the laser frequency ω_{exc} in the top layer of the film. From the calculated field intensity distribution in Fig. 1(a) and assuming that the value of the dipole moment in the tip-enhanced case does not differ significantly from the confocal case, we find that the excitation rate is enhanced in the near field by a factor of 4×10^4 as compared to the far-field excitation (see supplementary material [16]). The extra 15-times stronger PL intensity determined from the experiment then has to be explained by the influence of the tip on the PL yield of the film. Crystalline films of perylene chromophores like DIP have an exciton dispersion with a minimum at the surface of the Brillouin zone, resulting in a rather low PL yield in the percent range, or $\Gamma_{nr} \gg \Gamma_r$ [21]. This is different in the presence of the tip. According to Fermi's golden rule, the spontaneous radiative decay rate per frequency interval is $\frac{\partial \Gamma_r(\omega)}{\partial \omega} = \frac{2\omega}{3\hbar\epsilon}|\mathbf{D}_{em}|^2\rho(\omega)$, where $\mathbf{D}_{em}$ is the transition dipole for emission and $\rho(\omega)$ the photonic mode density along the tip axis. The tip increases locally the photonic mode density $\rho(\omega)$ in the gap between the apex and the DIP-film and thus increases the radiative recombination rate Γ_r.

Furthermore, the absorption by the tip provides an additional Γ_{nr} channel; both effects influence the PL yield. Hence, the extra 15 times stronger PL-intensity must be explained by a 15 fold increase of the PL-yield due to the tip with respect to the confocal far-field excitation, reflecting a 17 times enhanced Γ_r (supplementary material [16]).

An increased PL intensity along the terraces of a molecular crystal has never been observed before due to a lack of spatial resolution and sensitivity. Therefore, our results have to be discussed on the basis of bulk measurements averaging over large sample areas. *In situ* ellipsometric measurements of the complex dielectric function during the growth of pentacene films have revealed a blue shift in the imaginary part of the dielectric function in the first few molecular layers. Such a blue shift with respect to the bulk properties is a consequence of a reduced gas-to-crystal shift in the surface layer and results from a decoupling of the surface or edge molecules and their transitions from the underlying bulk material [22]. Therefore, their Γ_r should correspond more to a single molecule, far above the much slower Γ_r occurring in molecular crystals [23,24]. As a consequence, these molecules are expected to fluoresce independently. The red shift of the PL from step edges shown in Fig. 3(c) seems contradictory to the expected blue-shifted PL. However, we must not only consider the reduced intermolecular interactions at grain boundaries or surface edges, but also an enhanced tip-sample interaction. The energetic influence of an enhanced coupling between the Au plasmon and the DIP exciton-polariton seems to slightly outweigh other energetic influences on the molecular transition energy, giving a small red shift of the PL emission. The energetic shift of the transition energies at step edges leads to a further reduction of the exciton diffusion away from these sites, in keeping with a faster Γ_r arising from the molecular transition dipole. Within the ensemble of edge sites, the distribution over transition energies is influenced by geometric variations like the number of neighboring molecules. The intensity variations along the grain boundaries reflect the local disorder of the step edges, influencing, e.g., Γ_r and Γ_{nr}. Because of the anisotropic properties of the DIP film, the exciton diffusion length in the lateral and vertical directions can be different. Considering the lateral resolution of 17 nm achieved in our near-field imaging of the DIP film, we deduce that the upper limit of the DIP exciton diffusion length in the lateral direction should be comparable to this value. Otherwise, if the exciton generated by the tip-enhanced light field could diffuse away from the region probed by the tip, sharp PL imaging would not be possible. In addition, Kurrle *et al.* [4] have reported an exciton diffusion length of 100 nm along the direction perpendicular to the substrate. Because of the coupling between the tip plasmon and the DIP exciton polariton, we have a different situation since the Γ_r is speeded up so that the radiative lifetime τ_{rad} is reduced.

Therefore, we expect the 100 nm diffusion length to be shortened according to $L_{diff} = \sqrt{D\tau_{rad}}$, where D is the diffusion constant.

In conclusion, we have shown that tip-enhanced near-field optical microscopy with a parabolic mirror microscope reveals fine optical details correlated to the local film morphology and local spectroscopic information at the level of single molecular layers. The increased optical contrast and the nanometer spatial resolution at the molecular domain boundaries indicate an enhanced coupling between the tip plasmon and the exciton polariton in the molecular film, resulting in a 15-fold increased PL-emission yield. Our results open new perspectives for analyzing the local spectroscopic properties of molecular semiconductor films together with the local morphology at a spatial resolution far beyond the diffraction limit.

*alfred.meixner@uni-tuebingen.de
†dai.zhang@uni-tuebingen.de
[1] *Physics of Organic Semiconductors*, edited by W. Brütting (Wiley, Berlin, 2005).
[2] W. R. Salaneck *et al.*, *Conjugated Polymer and Molecular Interfaces: Science and Technology for Photonic and Optoelectronic Applications* (CRC Press, Boca Raton, 2001).
[3] A. C. Dürr *et al.*, Appl. Phys. Lett. **81**, 2276 (2002).
[4] D. Kurrle *et al.*, Appl. Phys. Lett. **92**, 133306 (2008).
[5] M. A. Loi *et al.*, Nature Mater. **4**, 81 (2005).
[6] C. Stanciu *et al.*, J. Microsc. **229**, 247 (2008).
[7] K. F. Domke *et al.*, J. Am. Chem. Soc. **128**, 14721 (2006).
[8] R. M. Stöckle *et al.*, Chem. Phys. Lett. **318**, 131 (2000).
[9] B. Pettinger *et al.*, Phys. Rev. B **76**, 113409 (2007).
[10] A. C. Dürr *et al.*, Phys. Rev. Lett. **90**, 016104 (2003).
[11] M. Sackrow *et al.*, Chem. Phys. Chem. **9**, 316 (2008).
[12] P. A. Temple and C. E. Hathaway, Phys. Rev. B **7**, 3685 (1973).
[13] R. Scholz and M. Schreiber, Chem. Phys. **325**, 9 (2006).
[14] V. Presser *et al.*, J. Raman Spectrosc. 40, 2015 (2009).
[15] U. Heinemeyer *et al.*, Phys. Rev. B **78**, 085210 (2008).
[16] See supplementary material at http://link.aps.org/supplemental/10.1103/PhysRevLett.104.056601 for detailed information.
[17] L. Gisslén and R. Scholz, Phys. Rev. B **80**, 115309 (2009).
[18] M. Heilig *et al.*, J. Lumin. **110**, 290 (2004).
[19] *Near-field Optics and Surface Plasmon Polaritons*, Topics Appl. Phys., edited by S. Kawata (Springer, Berlin, 2001).
[20] J. A. Porto *et al.*, Phys. Rev. B **67**, 085409 (2003).
[21] A. Nollau *et al.*, J. Appl. Phys. **87**, 7802 (2000).
[22] I. Vragović *et al.*, Eur. Phys. J. B **66**, 185 (2008).
[23] I. Vragović *et al.*, Phys. Rev. B **68**, 155202 (2003).
[24] A. Y. Kobitski *et al.*, Phys. Rev. B **68**, 155201 (2003).